Mechanism of behavior of two-way shape memory polymer at constant strain conditions

Andrés Posada-Murcia[§], Juan Manuel Uribe-Gomez[§], Stephan Förster[#], Thomas Thurn-Albrecht[§§], Jens-Uwe Sommer[†‡//], Kay Saalwächter[///], Eva Bittrich[†], Konrad Schneider[†], Martin Dulle[#], and Leonid Ionov[§*]*

[§]Faculty of Engineering Sciences and Bavarian Polymer Institute, University of Bayreuth, Ludwig Thoma Str. 36A, 95447, Bayreuth, Germany

[#]Jülich Centre for Neutron Science (JCNS-1/IBI8), Forschungszentrum Jülich, 52425 Jülich, Germany

[##]Jülich Centre for Neutron Science (JCNS-1/ICS-1), Forschungszentrum Jülich, 52425 Jülich, Germany

[§§]Institut für Physik - Polymerphysik, Martin-Luther Universität Halle-Wittenberg, 06120 Halle (Saale), Germany

[†] Leibniz Institute of Polymer Research Dresden e. V., Hohe Straße 6, 01069 Dresden, Germany.

[‡]Faculty of Physics, TU Dresden, Dresden, Germany.

[//]Cluster of Excellence Physics of Life, TU Dresden, Dresden, Germany.

[///]Institut für Physik - NMR, Martin-Luther-Universität Halle-Wittenberg, 06120 Halle (Saale), Germany

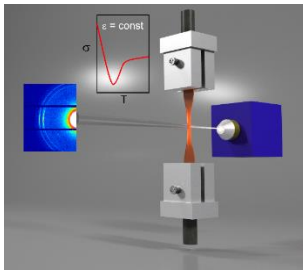

KEYWORDS: Shape-memory, crystallization, polymers, actuators, XRD, anisotropic structure.

ABSTRACT

In this paper, we report detailed investigation of structural changes occurring in two-way shape memory polymers (2W-SMP) upon thermal cycling at constant strain conditions. We demonstrate that cooling of stretched chemically crosslinked polycaprolactone results first in slow decrease of stress, the stress drops rapidly upon further cooling and further cooling results in sharp increase of stress. In this paper, we investigated structural changes occurring in each of these three phases using *in situ* force measurements and XRD analysis (SAXS and WAXS). In the first phase, the stress decreases due to decrease of entropic factor in elastic state. In the second phase, polymer chains start to crystallize in stretched state as result number of active springs producing stress decreases. This results in decrease of stretching degree of other polymer chains and finally, not stretched polymer chains crystallize that results in increase of stress – the polymer simply tends to shrink.

1. INTRODUCTION

Two-way shape memory polymers (2W-SMP) are promising kind of actuating materials due to their ability to actuate autonomously (without external power source) and reversibly with large amplitude in both wet and dry environments – combination of properties inaccessible to hydrogels, common shape memory polymers or piezoelectric polymers[1–6]. 2W-SMPs that actuate upon thermal cycling undergoing a reversible shape-shifting process can be separated in two classes: materials which require an applied stress for actuating, and certain ones which do not require it[7]. The 2W-SMPs of the first type consist of single component materials - crosslinked semicrystalline polymers, which change their length during crystallization/melting when an external force is applied and the polymer is stretched[8,9]. 2W-SMPs of the second kind are formed by two

fundamental structural elements: a scaffold, which plays a passive role in actuation and typically confers enhanced mechanical properties to the material, and a stretched crystallizing elastomer section, which enables the actuation[10–14]. The stretching of the elastic part is achieved during a shape-programming step and the passive polymer domains keep the elastic crystallizing component in a stretched state. Crystallization/melting of the stretched elastic component results in its elongation/contraction allowing a shape-shifting effect of the whole sample.

Several models were developed to explain and predict behavior of 2W-SMP. Chung *et al.*(2008) [15], for example, argued that elongation of stretched elastomer occurs due to oriented crystallization promoted greatly by the magnitude of the applied load. Moreover, Westbrook *et al.*(2010)[16] proposed a 1D model, which describes the coexistence of two phases during crystallization as the origin of two-way shape memory effect in semicrystalline polymers. The evolution of energy from an entropy governed-phase (rubbery state) to a stretched-induced crystalline phase during thermal cycling allows the reversible actuation of the material - strongly dependent on the rate of temperature change. A model based in the transition of free energy of a polymeric network under load subjected to crystallization from amorphous to crystalline domains was proposed by Dolynchuk *et al.* (2014)[17] and Kolesov *et al.* (2015)[18]. This approach correlates the free energy of crystallization- fold surface free energy of a crystal or lateral surface free energy for extended-chain crystal - and their orientation along the direction of the applied force with a sharp elongation of the material which is the essential driving force of reversible shape memory effect (SME). Validation of proposed models requires *in situ* experiments allowing a correlation between shape change and structural reorganization. Huang *et al* (2014)[19] performed *in situ* XRD experiments during crystallization-induced elongation confirming that the length of polymer subjected to a

constant external load changes while it crystallizes. Meanwhile, a detailed evaluation of the correlation between crystallinity and orientation degree with elongation has not been performed complicating the validation of these models.

Although, the behavior of 2W-SMP at constant stress conditions is relatively well studied, most of 2W-SMP are used in setups where they undergo out of plane deformation such as bending and twisting[20–25]while the length of whole sample remains nearly unchanged during actuation. This means that such polymers are used in different conditions than 2W-SMPs which require an external constant force to actuate. Recently, we published a phenomenological comparison of behavior of 2W-SMP in both regimes[26]: in constant stress setup polymer undergoes sharp elongation right before crystallization while in constant strain setup the stretched polymer undergoes an anomalous sharp drop of stress right before crystallization followed then by an expected increase of measured stress upon further cooling. The discussion of the mechanism and behavior of polymers in constant strain mode in thermal cycling remained out of the scope of our paper. In this paper we undertake an attempt to reveal processes occurring in semicrystalline polymers by performing *in situ* XRD studies of stretched crosslinked PCL in constant strain setup upon cooling, accompanied by simultaneous measurements of extensional stress in polymer.

2.EXPERIMENTAL SECTION

2.1 Materials. Commercially available PCL (Mn = 80kDa), dicumyl peroxide (DCP) (98%) and chloroform (99%) were purchased from Sigma-Aldrich and further used as received without any additional treatment/processing.

2.2 Preparation of samples. PCL beads were dissolved in chloroform before being mixed with 5wt% of DCP at room temperature (PCL DCP 5%). After proper homogenization the viscous solution was poured and let to dry overnight on a flat glass recipient obtaining a homogeneous solid film from which 10 x 8mm rectangular pieces (average thickness of 0.7mm) were cut. Finally, the probes were thermally cross-linked in a vacuum oven for 2h at 160°C.

2.3 Thermomechanical cycle under constant strain and constant stress. Evolution of extensional stress during thermal cycling at constant elongation was performed, a typical run is described as follows: PCL film is clamped and extended on molten state (70°C) up to a given strain, 200% e.g. Then, stretched samples were cooled to ca 25°C. Finally, the crystallized probes were heated again up to molten state, cooling/heating steps of 1°C min^{-1} were used. Strain progression on constant stress experiments was studied by applying an analogous thermal cycle as mentioned above. The value of constant stress to extend a specimen by ca 200% was obtained from the constant strain experiment while the TW-SME was demonstrated (**Figure 1**).

2.4 Kinetic study of un-stretched/stretched PCL crystallization process. Time dependent analysis of observed stress drop in constant strain experiments upon cooling and its correlation with stretching degree was carried out. Slow cooling program was implemented on stretched cured polymer and described as follows: Specimens were cooled from molten state (70°C) to 55°C on a 30min window, followed by -1°C cooling and subsequent annealing steps for 15 and 30 minutes correspondingly until 40°C, these temperature limits are supported on our previous observation of the transient state occurrence where the stress drop is detected. Unstretched and not crosslinked samples were tested as a reference (**Figure 2**). Additionally, we performed constant strain thermal-analysis of the PCL DCP 5% sample and evaluated force evolution as a function of the applied

cooling/heating rate (0.5, 1 and 2°Cmin^{-1}) using a homologous program as described above (**Figure S1**).

2.5 Differential Scanning Calorimetry (DSC). Thermal analysis of uncross-linked and cured PCL specimens was performed using a DSC3 (Mettler Toledo, USA). Samples were subjected to a three step program: First heated from 0 to 200 °C then, cooled from 200 to 0 °C and finally heated again from 0°C to 200 °C at a heating-cooling rate of 1°C min^{-1} under nitrogen atmosphere (**Figure 2**).

2.6 Crossed polarizers experiments. Qualitative study of crystallization at constant strain of stretched PCL DCP 5% was carried out using crossed polarizers. Two light polarizers were mounted with a 90° disposition on a self-made device equipped with a LED white light panel, movable clamps which allowed the extension of the specimen above the light source and a heating unit. Probes were fastened and subsequently heated to molten state ~70°C, then the polymer was extended up to 200% of its original length and fixed as the heating was maintained. At this point, the heating was stopped to allow crystallization of the material while recording temperature. Birefringence changes on the sample were noted and registered along its cooling to room temperature (**Figure 3**).

2.7 *In-situ* wide-angle and small angle X-ray scattering analysis (WAXS and SAXS). Scattering patterns were recorded with the SAXS system "Ganesha-Air" from (SAXSLAB, Xenocs). The X-ray source of this laboratory-based system was a D2-MetalJet (Excillum) with a liquid-metal anode operating at 70 kV and 3.57 mA with Ga-Kα radiation (λ = 0.13141 nm) providing a very brilliant and a very small beam (<200 μm). The beam was focused with a focal length of 55 cm using a specially made X-ray multilayer optic (Xenocs) to provide a very small and intense beam at the sample position.

The pre-stretched samples (200 and 300% of their original length) where placed in a Linkam TST-350 tensile stage with the glass windows replaced with 10µm thick mica windows. All samples were prepared in the same way for the measurement. After fixing the heat pressed samples on the stage the blocks where moved apart until a force value of 2Nm was reached. This was done to ensure good contact of the sample with the heating block as well as to have a standardized starting point. This is especially important as it was unavoidable to make two separate measurements for WAXS (0.16m distance) and SAXS (51cm) with two separate samples.

Each sample was heated and kept at 70°C for 5min. After that, the sample was cooled down with a cooling rate of -1°C/min while being continuously illuminated with X-rays. The scattering was recorded continuously and a separate pattern was saved every 15s for the duration of the cool down. Details to the different data reduction procedures as well as the analysis of the data are given in the supporting information.

3. RESULTS AND DISCUSSION

For our experiment we used chemically crosslinked PCL with an initial molecular weight Mn = 80 kDa. The stretched polymer demonstrated the typical change of stress upon crystallization made at constant strain conditions – stress sharply drops upon cooling and then increases (**Figure 1a**). The change of length upon crystallization under constant stress also has typical character – the sample undergoes sharp elongation upon cooling followed by a recovery of original length upon heating (**Figure 1b**).

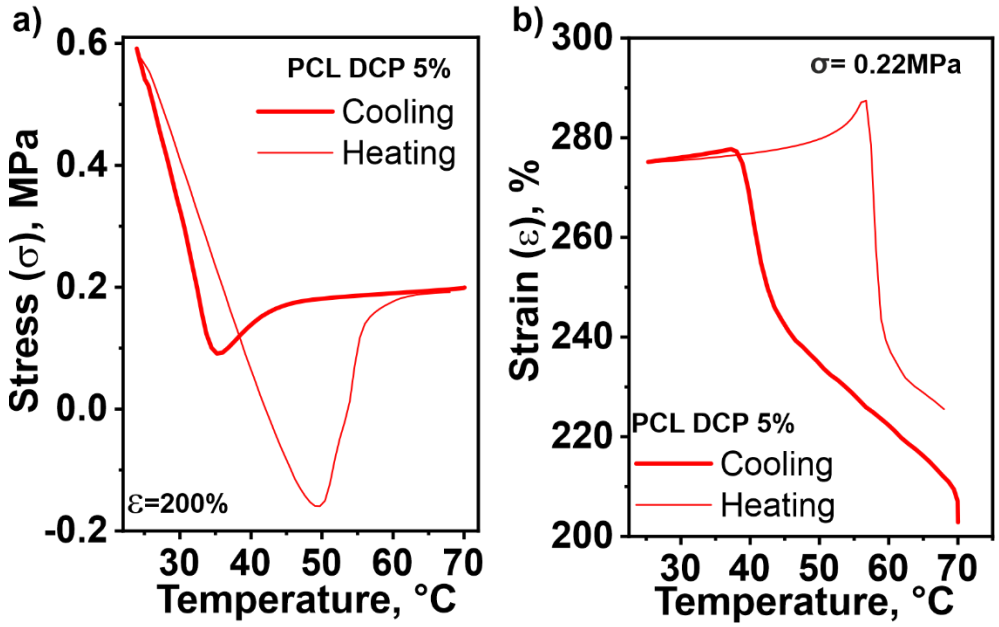

Figure 1. *Behavior of crosslinked PCL in (a)– constant strain and (b)– constant stress experiments.*

Kinetic evaluation of crystallization process under constant strain. In order to understand the stability of the transient state upon cooling associated with the stress drop at constant strain, we performed crystallization essays at very slow cooling rate. We first made DSC of not stretched crosslinked and not crosslinked polymers at very low rate ($1°C \cdot min^{-1}$) to identify the onset of crystallization. It was found from DSC that the onset of crystallization is observed at 40-42°C while, the crystallization peak is located at ca 35-37°C (**Figure 2a**). Next, we measured force generated by polymer at very slow cooling rate – the temperature was reduced stepwise by – 1°C each step followed by a 30 min annealing at constant temperature. The experiment was carried out with stretched crosslinked polymers as well as with a non-stretched crosslinked sample and a not crosslinked probe as references. It was observed that the elastic storage modulus of not stretched crosslinked and not crosslinked polymers starts to increase at ca 47°C- 48°C (**Figure 2b**). The

increase of the storage modulus (E') becomes considerable at 45-46°C. The difference in the temperature of crystallization onset provided by DSC and DMA is caused mainly by sensitivities of methods. DSC is sensitive to changes on volume/mass of crystallizing materials – formation of a small number of crystallites is not detectable by DSC. On the other hand, DMA is sensitive to the number of small crystallites, which act as physical crosslinking points increasing the value of elastic modulus of elastomers[27].

We plotted the evolution of temperature and stress of the stretched crosslinked polymer with time (**Figurec**) as well as slope of stress/time curve (first derivative) vs time (**Figured**) to study the kinetics of the transition. We observed that changes of stress ($\Delta\sigma$) in each cooling step and during annealing remain nearly constant upon cooling from 55°C to 52°C. The stress is changing linearly with time during annealing, which means that the relaxation time is over 30 minutes as the sample remains at a constant temperature. At 52°C, we observed an intense decrease of stress resulting in larger values of $\Delta\sigma$ that became more pronounced for each cooling-annealing step as depicted on **Figure 2e**. As result, stress vs time curve becomes steeper. At 47°C an increase of the stress was observed. Very sharp changes of stress were observed in each step of cooling. Annealing after each cooling step resulted in relaxation of stress as it tended to approach an equilibrium level. The value of stress at equilibrium, which can be achieved in each annealing step, increases with decreasing temperature. The main observation of this experiment is that the transitional state corresponding to the stress drop on stretched polymers at constant strain upon cooling is stable through time – we observed the stress drop over a period of ca 3 hours.

We performed a control experiment to investigate the effect of temperature on the stress drop transitional state (**Figuref**). For this we performed the crystallization of a stretched sample fixed at 200% of its original length and recorded the evolution of stress with temperature upon cooling. It was observed that stress started to rapidly drop at ca 45°C. The temperature was further reduced down to 37°C, which is lower than the temperature, at which an increase of stress during step-wise cooling was observed, and annealed at this temperature. The stress continued to further decrease at 37°C and then increased upon annealing at this temperature. This experiment demonstrated that the transitional state is not strictly determined by temperature but corresponds to an intermediate structure adopted by polymer chains upon transition from amorphous to crystalline states and cannot be avoided at the conditions at which crystallization occurs.

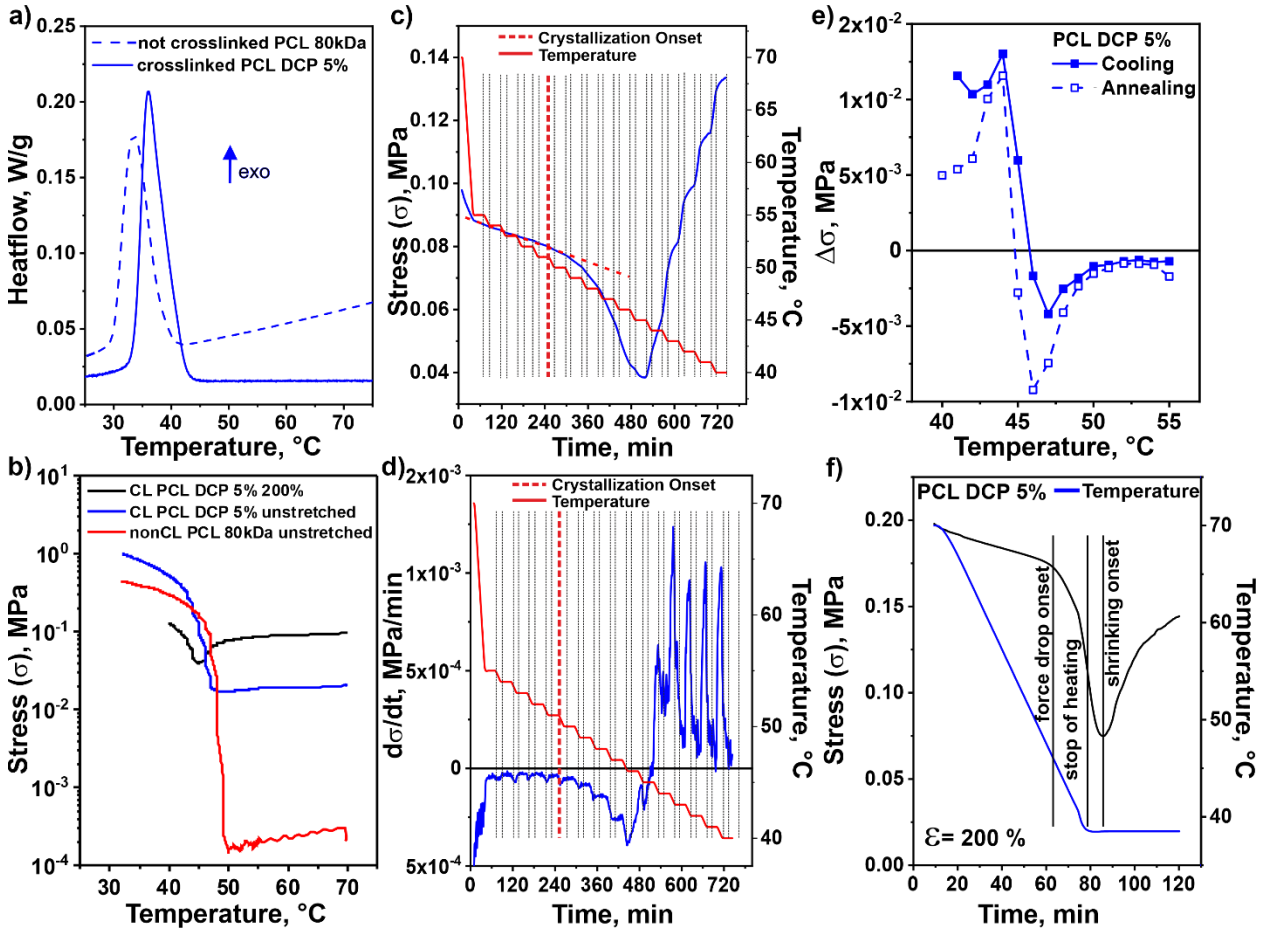

Figure 2. *Kinetics of stress evolution upon cooling: (a)– DSC of crosslinked and not crosslinked polymers at 1°C ·min^{-1}; (b)– evolution of stress with temperature of not stretched polymers – 1°C each 30min (c)– evolution of stress with time of stretched polymer during cooling; (d)– evolution of the slope stress vs time with temperature of stretched polymer during cooling; (e)– stress drop in each step of cooling and annealing; (f)– evolution of stress with time during slow cooling and annealing at constant temperature below temperature of onset of crystallization.*

In-situ SAXS and WAXS structural analysis. 200% elongation. We studied the structural evolution of stretched elastomers with 200% of elongation upon cooling and crystallization by performing *in situ* SAXS and WAXS measurements at constant strain (**Figure 3**). Obtained SAXS patterns showed that the polymer is fully amorphous at 70°C (**Figure 3a, b**). Decrease of temperature to 58°C results in appearance of anisotropic scattering at low q which is usually attributed to density fluctuation[28–32] . However, the fact that this signal at low q is showing a very strong orientational anisotropy right from the start is remarkable. This can be described by an anisotropic spinodal decomposition[33]. This behavior has been reported already for PCL upon cooling[34]. The crosslinked points located within the amorphous regions of the sample have a slightly different density than the rest of the polymer acting as the driving force for the decomposition. The first discernable SAXS signal shows up at 58°C and at the point when stress starts to drop at 53°C (**Figure S2**), we observed the appearance of meridional spots on the 2D SAXS pattern at q=1.2nm^{-1}, which indicates the inception of well-defined oriented lamellae. Upon further cooling a structure factor peak in the meridional direction is developing from stacking of the lamellae as well as continuous increase of scattered intensity (**Figure 3a, b**). At ca 43°C the minimum of force was observed, total force drop was ca 9%. Below 42°C an isotropic scattering contribution about 100 times weaker than the signal on the meridian shows up on the equator. This ring is also a structure factor

peak from lamellae but this time from the ones not oriented in any particular direction. Although weak in intensity we were able to fit the data well to the same model as the oriented lamellae.

WAXS analysis of the stretched sample showed no observable reflections between 70 and 54°C, indicating no crystalline phase in this temperature range when the stress versus temperature curve remains linear. However, the appearance of an azimuthally anisotropic reflection at 53°C evidently indicates the onset of the formation of an oriented crystalline phase (**Figure 3a, c; Figure S3**) as the force starts to fall. Thus, measured crystallinity starts to increase while the sample is furtherly cooled. The degree of crystallinity is ca10% at the point of minimum force, which corresponds to a 10% drop in force in relation to the force in elastic regime. Further cooling to 37°C results in appearance of (110) isotropic reflection[35], which could be related to massive formation of disordered crystallites, provoking a sustained further arising of the detected crystallinity until the cooling program is over (**Figure 3d**).

A Voigt profile fitting model was applied to the obtained SAXS and WAXS azimuthal plots. Azimuthal fitted WAXS profiles of 200% stretched crosslinked PCL revealed that peak's position and width parameters are hardly changing upon cooling (**Figure S4**). On the contrary, the evolution of the height parameter with temperature follows the same two stage behavior as the simultaneously recorded force (**Figure 3d**). From 53-40°C – where the fall in force takes place - the peak's height is rapidly growing to about 80% of its final height. Between 40 to 30°C the height parameter grows modestly while the recorded force increases for both small and wide-angle scattering data.

The contribution of the oriented crystalline domains to the intensity of the peak's height for SAXS and WAXS measurements was assessed by subtracting the offset criterion - which in an azimuthal plot is a constant (angle indepemdent) background – from the overall height signal. The resulting values and their correlation with the measured stress upon cooling revealed that on the temperature range, where the stress drop is recorded the intensity of oriented crystalline phase grows sharply until the force minimum is reached (ca 43°C). Below this temperature the progression of the signal becomes monotonous demonstrating that the further increase exhibited by the overall height parameter between 42 and 30°C is solely a contribution of the offset criterion to the intensity of the peak as depicted on **Figure 3d**. This observation is way more evident on WAXS experiments as they are carried on a shorter length scale and its signal correspond to the crystal lattice while SAXS peaks do not answer to a such well-defined structure and are susceptible to slightly shift positions with temperature due to the change in concentration as well as separation distance.

Therefore, these observations allowed us to associate the anomalous thermomechanical behavior of constantly strained polymers upon cooling with the existence of two different types of crystalline phases on the crystallization process: oriented or with certain degree of orientation and non-oriented crystalline domains. As the stretched material leaves the rubbery amorphous state (70-54°C) and enters the transient regime characterized by the stress drop (ca 53°C) a highly ordered crystalline phase begins to grow until the force minimum is reached (around 43°C for 200% strained PCL), signal intensity for both SAXS and WAXS grows sharply as a consequence of this process. Finally, below 42°C the measured force rises as the offset parameter becomes the main contribution to the intensity of the acquired small and wide-angle scattering signals due to unordered crystalline phase formation as depicted on **Figures 3d and S5**.

We have also observed the stretched polymer sample in crossed polarizers (**Figure 3e**). The temperature measurements were imprecise and results can be used for qualitative illustration of process occurring in the polymers. In crossed polarizers, the stretched polymer at 65°C exhibits a yellowish coloration indicating birefringence of the stretched polymer chains. Cooling the sample under constant strain leads to a reddish to bluish color change in some areas of the sample, which, according to the Michel-Levy diagram, indicates an increase in birefringence[36]. This implies an increase in optical anisotropy and, therefore, the degree of orientation of the polymer chains. As the temperature further decreases, the sample becomes slightly hazy, presumably due to massive crystallization. Finally, at 30°C the sample becomes completely white and opaque.

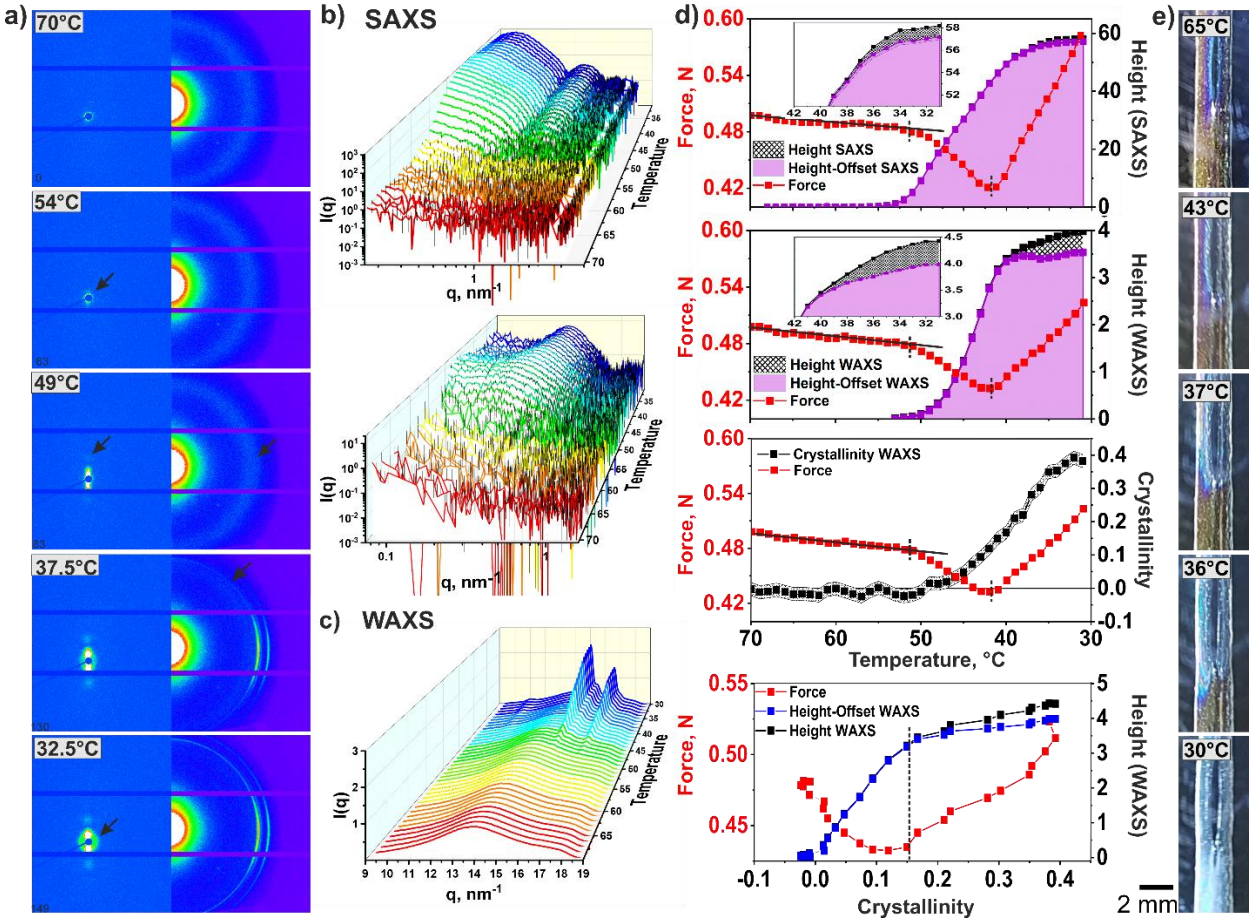

Figure 3. *In-situ structural studies of 200% stretched crosslinked PCL: (a) – 2D SAXS (left) and 2D WAXS images (right); temperature evolution of (b)– SAXS and (c)– WAXS radial patterns; (d)– evolution of SAXS and WAXS height and height-offset Voigt fitting parameters and degree of crystallinity with temperature as well as dependence of WAXS Voigt parameters with force on degree of crystallinity; (e)– crossed polarizer images.*

300% Elongation. We studied effect of stretching degree on evolution of structure of stretched polymer upon its crystallization. Generally, behavior of stronger stretched polymer (300 %) is qualitatively similar to discussed above. The main effects of stretching are that at 70°C the SAXS 2D pattern shows already a modest anisotropic reflection corresponding to slightly oriented platelets (**Figure S6**). Accordingly, the WAXS experiments revealed the inception of an

anisotropic reflection ca 60°C. The outset of reflections denoting orientation occur at higher temperatures for more stretched samples. This trend continued its course with further cooling developing the same pattern of reflections previously described for less-strained probes (**Figures S6-7**). Even more, a sharper stress drop takes place at higher temperature (ca 46°C) exhibiting a force reduction of 15% while crystallinity at force minimum is also ca 15% - stress drop corresponds to degree of crystallinity as in the case of polymer stretched to 200%. This results are in complete agreement with the observations reported on our previous study and provides an explanation for the anomalous recorded stress drop caused by the onset of crystallization process on constant strain mode and its dependence on stretch degree. Voigt fitting of azimuthal profiles and the associated height and offset parameters for 300% stretched samples followed an analogous evolution upon cooling suggesting the same two-stepped crystallization course than less stretched specimens but taking place at higher temperatures (**Figure S6 and Figure S7**). As a final remark, must be noted that offset's contribution to the overall SAXS and WAXS intensity for 300% stretched samples is less significant than for 200% PCL as a consequence of the enhancement of oriented crystallization on a greatly strained probe.

SAXS Form and structure factor fitting. A simple homogenous disc form factor[37] was used to describe the acquired small-angle scattering of the radially averaged signal for stretched PCL up to 200 and 300% upon cooling under constant strain. For the radial average a cone shape region of interest was used encompassing an angle of 20° to only capture the signal from the oriented platelets on the meridian. The scattering intensity is calculated for a flat radially averaged cylinder. We use the fact that we only radially averaged over the ROI to use the form factor without preferred orientation to fit the data.

$$P(q) = \frac{scale}{V_{cyl}} \int_0^{\pi/2} f^2(q,\alpha) \sin\alpha \, d\alpha \quad (1)$$

$$f(q,\alpha) = 2(\rho_{cyl} - \rho_{sol}) V_{cyl} j_0(qL_{enght} \cos\alpha) \frac{J_1(qr_{adius} \sin\alpha)}{(qr_{adius} \sin\alpha)} \quad (2)$$

$$V_{cyl} = \pi r^2 L \;\; and \; j_0 = {\sin x}/{x} \quad (3)$$

Where J_1 is the first order Bessel function; r is the radius and L is the thickness of the disc.

As cooling progressed the scattering not only showed the features of a disc form factor but also a structure factor from a stacking disc arrangement along the polymer chains stretching orientation, this can be seen in the obtained scattering data as a peak developing towards low q values (**Figure S7**). To fit this data, we introduced a lamellar structure factor to model the stacked disc conformation. In this case we used the radial structure factor S(q) in powder average of a crystal lattice including the Debye-Waller factor and broadening due to domain size. The scattering for a crystalline domain in the powder average is:

$$I(q) = nP(q)S(q) \quad (4)$$

With n being the number density; P(q) the disc form factor and S(q) the structure factor.

The structure factor is:

$$S(q) = 1 + \beta(q)(Z_0(q) - 1) * DW(q) \quad (5)$$

With $\beta(q)$ as the asymmetry factor depending on the scattering amplitude and the particle polydispersity, $Z_0(q)$ is the lattice factor describing the spatial distribution of particles, DW(q) as the Debye-Waller factor.

A more detailed description can be found in Förster *et al*[38]. The code to calculate the scattering is included in Jscatter[39] which was used to fit and process all scattering data in the manuscript.

In the case of the sample elongated to 200% the first discernible signal shows up around 58°C, from 58 to 50°C a model without structure factor suited well to fit the data. The threshold of 49°C, where the introduction of structure factor was necessary, falls together with the detected decrease in force measured alongside the SAXS data. It was also observed that on the temperature range between 58 to 50°C from all the fitted parameters only the scale parameter - which corresponds to the concentration - is significantly increasing while the thickness and polydispersity of the discs stayed constant **(Figure 4a)**.

The data below 50°C needed the incorporation of a structure factor model. From this point onward the thickness and polydispersity were kept constant to ensure a faster and more stable fitting since during the remaining course of the test we found that these parameters exhibited no significant change as temperature was lowered. The structure factor yields mainly two parameters: The distance describing the separation between platelets as well as the domain size for a lamellar crystal.

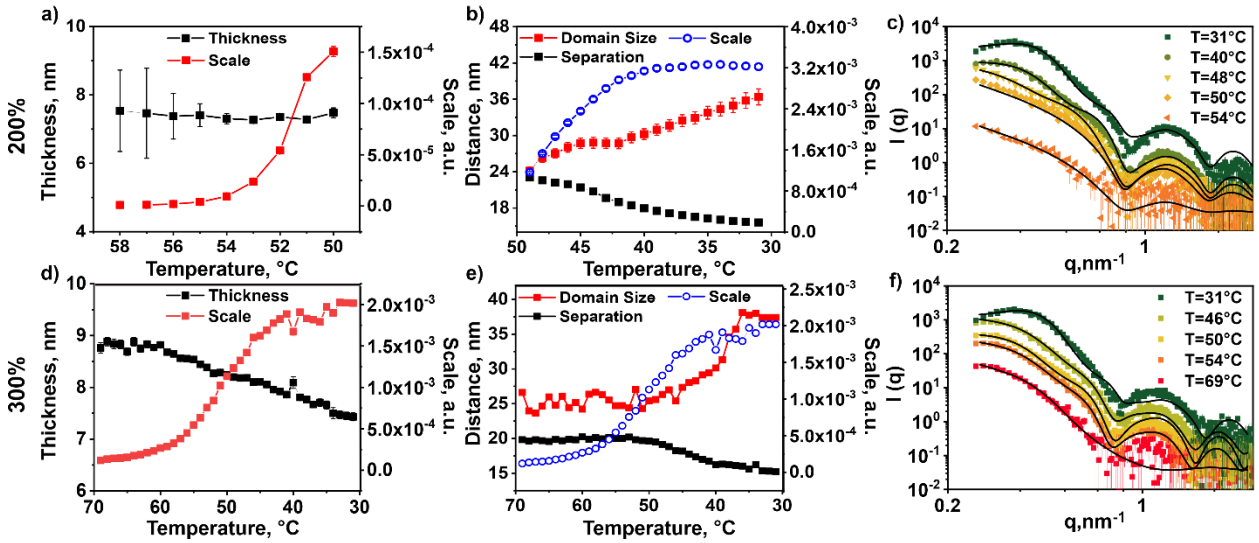

Figure 4. *Form and structure factor fitting study of 200% (a)–Thickness and scale parameters from disc form factor fitting; (b)– separation distance, domain size and scale from stacked disc structure factor fitting; (c)– Data and fits from form and structure factor models and 300% stretched PCL upon cooling (d)–Thickness and scale parameters from disc form factor fitting; (e)– separation distance, domain size and scale from stacked disc structure factor fitting; (f)– Data and fits from form and structure factor models; (c,f) the data and fit for 31°C was shifted on the y-scale by a factor of 5 for better visibility.*

The increase in domain size together with the decrease in platelets separation distance below 50°C (**Figure 4b)** is the result of the increase of order within the polymer chains above the 10nm size regime. One can understand this behavior the following way: The packed stacks of platelets are solidifying thereby decreasing their separation distance and as a side effect the order within the stacks is increasing which is reflected in the domain size parameter evolution. Overall the applied model could fit the radial averaged data in the meridional direction very well with the smallest amount of possible fit parameters (**Figure 4c**), a full table with all parameters for all temperatures and samples is provided on SI (Table S1-S4).

For the 300% PCL sample the fitting was done the same way as for the 200% sample with the only difference being that structure factor was included for all investigated temperatures (**Figure 4d-f**). The trends we see here are the same as for the 200% sample but the final domain size is a little larger and even at 70°C the sample has not fully lost its orientation and still clearly shows oriented spinodal decomposition.

Non oriented platelets (equatorial scattering). As mentioned earlier a noticeable isotropic scattering contribution is showing up below 42°C in SAXS as well as in WAXS (Fig. 3a). We attribute this signal to non-oriented but still crystalline lamellae. Again the 300% sample shows this signal at a slightly higher T than its less stretched counterpart. In WAXS it is pretty clear that the ring comes from to the same crystal structure as the main signal as all peak positions in q are the same. For SAXS however there could be several reasons for such behavior, the two most likely are: (I) A structure factor peak due to spatial correlations of the oriented lamellae due to their high relative concentration and close proximity. (II) The same kind of structure factor from stacked lamellae as in the meridional direction but this time without preferred orientation. The first would give only the structure factor without any form factor contribution in the equatorial direction and the second type would give both but with different structural parameters such as thickness or domain size.

When radially averaging on the equator we got the same type of scattering as for the meridional direction: stacked lamellae, but about a hundred times weaker in intensity as depicted on **Figure 5a**. We were able to fit these curves with the same model as the oriented platelets. The difference

we see in thickness as well as domain size come from the constant strain conditions in which the experiment was conducted, these non-oriented lamellae are less strained and therefore not as stretched as the oriented ones. For instance, the platelets in equatorial scattering are thinner (~6nm) than the ones on the meridian- with a thickness of ~7.5nm- for the same sample (**Figure 5b**). The domain size is similar for both oriented and non-oriented stacks but slightly larger for the 300%, even for non-oriented stacks as shown on **Figure 5c**. Details on the mechanism behind this behavior is discussed on the next paragraph.

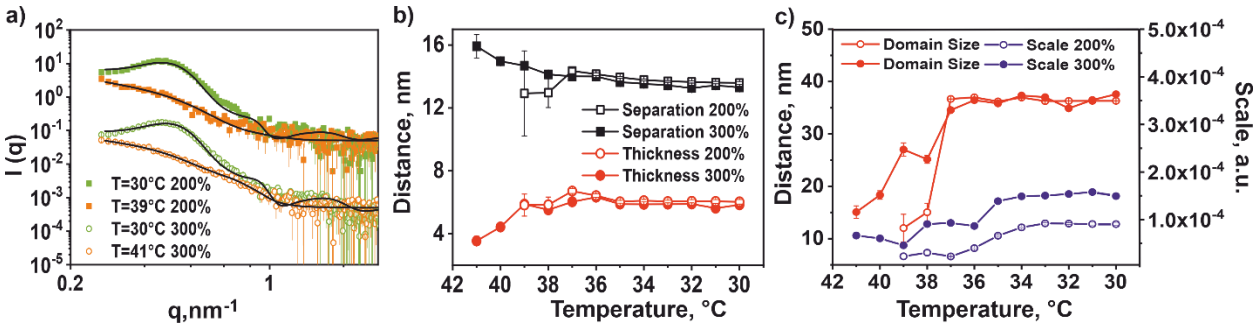

Figure 5. *Form and structure factor fitting study of radially averaged equatorial scattering for 200% and 300% stretched PCL (a)– Data and fitting plots from form and structure factor models, data and plots for 300% sample was shifted on the y-scale by a factor of 100 for better representation (b)–Thickness and separation distance from stacked platelets form factor fitting; (c)– Domain size and scale from stacked disc structure factor fitting.*

Crystallization mechanism of semicrystalline crosslinked polymers under constant strain. Thus, the stretched polymer undergoes the following stages during crystallization: (i) formation of oriented crystallites that is associated with stress drop followed by (ii) formation of unoriented crystallites that is associated with stress growth. We propose the following scheme for process of crystallization under constant strain. The crosslinked polymer in amorphous state is presented in

the form of springs (chain strands) connected in series and in parallel as depicted on **Figure 6**. The knots, where springs are connected, are crosslinking points. For simplicity, we just connected four springs. All springs are initially uniformly stretched under mechanical load and allowed to crystallize under constant strain (**Figure 6a**) and constant stress conditions (**Figure 6b**). Crystallization of stretched chains on both cases shall start at higher temperature than crystallization of not stretched ones since their conformation is closer to a crystallized chain. Cooling down the constantly strained spring-framework results in crystallization of one strand – it folds and forms stretched oriented lamellas under applied external force. The number of elastically active strands decreases modifying the stress distribution along the network. Therefore, the strand parallel to crystallized one is unable to resist the produced conformational-tension which results in its stretching while the two remaining strands contract freely as they are not subjected to constant force (**Figure 6a**). Totally stress is further reduced and character of stretching of polymer chains keep changing. Next, second strand, which is parallel to already crystallized one, crystallizes as it became even more stretched. First and second strands form oriented lamellas. Two remaining strands contract even stronger in the absence of resistance produced by extended chains and crystallize with formation of unoriented lamellas. Exactly this scenario was observed – degree of orientation of chains and lamellas increased in the beginning of crystallization and decreased in the final stage of crystallization.

Using this simplified four-spring model we estimated how force acting on the ends of this construct changes if one spring is removed. We consider that the four-spring construct was stretched, the absolute elongation is Δx. The elongation of each half is then $\Delta x/2$. The total force produced by construct is a sum forces produced by each of four springs $F^o = 4k\frac{\Delta x}{2} = 2k\Delta x$. Imagine, one of

springs is removed. Then, a spring, which is parallel to removed one, extends – it elongation is Δx_1, two others contract – their elongation Δx_2. The force produced by extended spring is $F_1 = k\Delta x_1$ and force produced by two contracted springs $F_2 = 2k\Delta x_2$. Both forces are equal at the point of equilibrium $k\Delta x_1 = 2k\Delta x_2$. Considering that $\Delta x_1 + \Delta x_2 = \Delta x$ because the total length remains unchanged, we get $\Delta x_2 = \frac{\Delta x}{3}$ and $\Delta x_1 = \frac{2\Delta x}{3}$ and the total force $F' = F_1 + F_2 = \frac{4}{3}k\Delta x$ that is lower than F^o, $\Delta F = F' - F^o = \frac{4}{3}k\Delta x - 2k\Delta x = -\frac{2}{3}k\Delta x$. In general case, when both sets consist of n springs and m become inactive in one set, the force drop is $\Delta F = F' - F^o = 2n\left(\frac{(n-m)}{2n-m} - 0.5\right)k\Delta x$

This model provides qualitative explanation to facts reported in our previous paper[26]. First, it is necessary to increase the degree of chain stretching (increase stress in the elastic state) in order to increase the stress drop - the more the chains are stretched, the larger is elastic force provided by each strand and the greater the stress drop will be, which is confirmed by the experimental results published in the previous article. The increase of stress in elastic state will cause more strands to crystallize in the stretched state meaning that the onset of stress drop shall be observed at higher temperature that was also observed experimentally. As result, the number of strands, which crystallize in relaxed state, must be lower that shall reduce the stress increase upon further cooling that was also observed experimentally. The made conclusion allows us to assume that the largest stress drop shall be observed when polymer chains are completely stretched in elastic state. The maximal degree of stretching scales linearly with square root of number of monomer units in a polymer strand. In this case, the stress must drop to zero upon crystallization and no further increase of stress at low temperature must be observed because all chains crystallize in stretched

state. A summary of the previously mentioned findings and their explanation for the unexpected crystallization behavior of semycrystalline polymers upon constant strain is presented on **Figure 6c.**

In constant stress experiment, the scenario is slightly different. Crystallization of single strand causes redistribution of stress and as result the strand, which is parallel to crystallized one, elongates (**Figure 6b**). The length of two other does not change because stress is constant. Afterwards, another strand crystallizes that results in further extension of parallel strand under applied stress. As results all strands shall crystallize in stretched state and the degree of orientation of chains must be larger than that in constant strain experiment. The visual analysis of 2D WAXS patterns obtained by Huang *et al*[19] provide the experimental evidence for this.

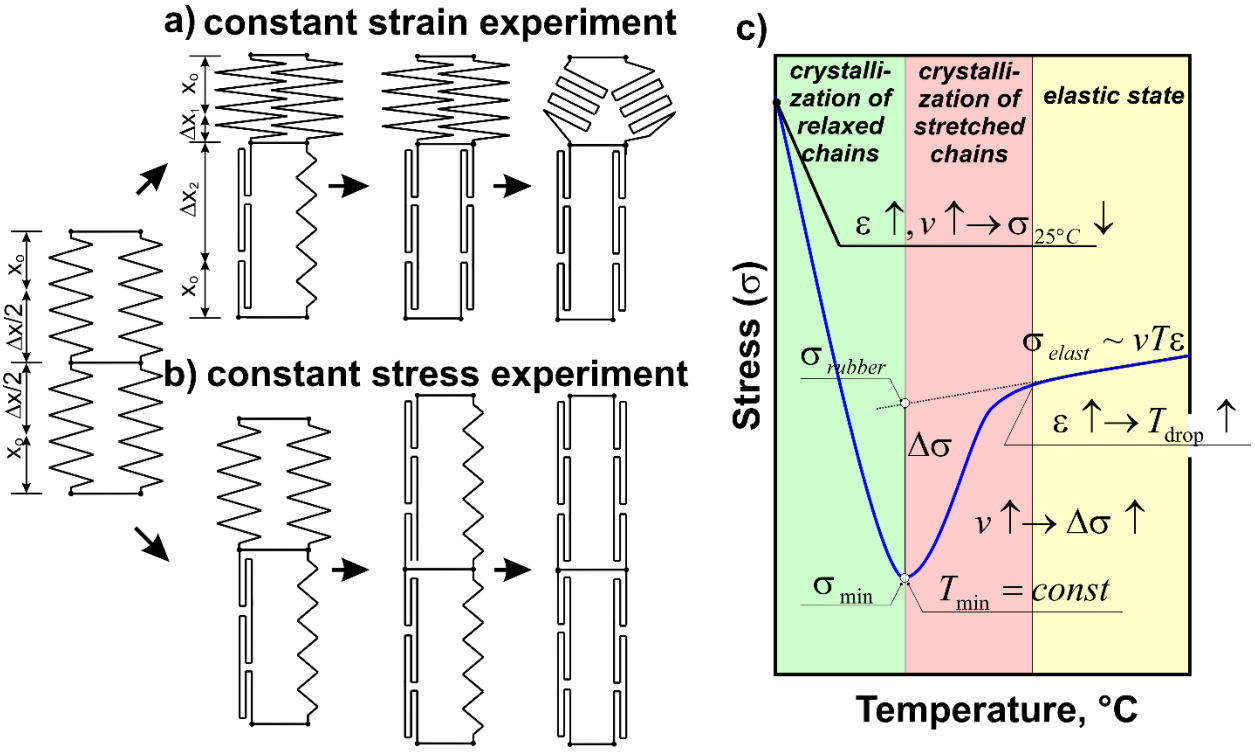

Figure 6. *Schematic representation occurring in stretched crosslinked elastomers upon their crystallization in (a)– constant strain and (b)– constant stress experiments. (c)– Summary of findings for constant strain experiments upon cooling.*

CONCLUSIONS

In this study we carried out a detailed research on the mechanism and characterization of the behavior of reversible shape memory effect of crosslinked PCL on constant strain mode upon cooling. We demonstrated by performing a thorough kinetic study on the crystallization of stretched polymer with very slow cooling/annealing steps that the transient state which leads to the observed stress drop ($\Delta\sigma$) happens to be a stable intermediate phase structure adopted by polymer chains upon transition from amorphous to crystalline state. The stability of this phase was proven to be not strictly conditioned by a further decrease of temperature.

SAXS and WAXS measurements together with a Voigt fitting analysis of the corresponding azimuthal profiles allowed us to determine that crystallization process occurs on a two-step course where two families of crystallites could be identified. As the stress drop is recorded a highly orientated crystalline phase is detected while the intensity of the signal height rapidly grows to ca 80% of its final height until the force minimum is reached. Further cooling leads the measured force to arise although ordered crystallites contribution to signal's height parameter becomes monotonous from this point - indicating the outset of non-oriented crystalline domains supported on a sharp increase of the offset criterion. It was also found that width and peak position parameters are barely changing on the course of the crystallization process. The afore mentioned observations were also noted for even highly stretched PCL samples though their manifestation occur at higher

temperatures. Higher strain degree of the sample leads to a sharper stress drop which is proportional to the ordered crystalline phase contribution to the crystallinity degree.

A rigorous form and structure factor fitting study carried out with the collected SAXS data showed an outstanding correlation with a form factor from orientated platelets and a structure factor from a stacking disc arrangement on the meridional direction while the cooling was following its course. It was noted that the isotropic equatorial scattering -observed on 200% and 300% PCL stretched samples- sets in at the same temperature where the minimum of force was recorded; the radial averaging of equatorial response fitted properly with a structure factor from non-oriented stacked lamellae corroborating a two-stepped crystallization process.

Finally, these observations allowed us to propose a model for the crystallization process on constant strain mode which provides reasonable explanation to previously reported anomalous behavior. Stretched polymer chains crystallize first from molten-elastic state producing a redistribution of stress upon the polymer network which leads to the elongation and further crystallization of parallel-neighboring strands- anomalous stress drop. As the length of the sample remains constant, relaxed polymer chains contract and crystallize forming unoriented lamellas increasing the measured force upon further cooling.

ASSOCIATED CONTENT

Supporting Information

HERE GOES THE NAMES OF THE SCHEMES AND TABLES OF SI (waiting for Martin)

AUTHOR INFORMATION

Corresponding Authors

Leonid Ionov

* E-mail: leonid.ionov@uni-bayreuth.de

Martin Dulle

* E-mail: m.dulle@fz-juelich.de

Author Contributions

The manuscript was written through contributions of all authors. All authors have given approval to the final version of the manuscript.

Funding Sources

The authors are grateful to DFG for financial support (grants IO 68/10-1 and IO 68/11-1, SO 277/18-1).

Notes

The authors declare no conflicts of interest.

ACKNOWLEDGMENT

Here the acknowledgments

ABBREVIATIONS

2W-SMP, two-way shape memory polymers; PCL, poly(ε-caprolactone); SME, shape memory effect; DCP, dicumyl peroxide; DSC, differential scanning calorimetry; XRD, X-ray diffraction; WAXS, wide-angle X-ray scattering; SAXS, small angle X-ray scattering

REFERENCES

(1) Kaczmarek, H.; Królikowski, B.; Klimiec, E.; Chylińska, M.; Bajer, D. Advances in the Study of Piezoelectric Polymers. Russ. Chem. Rev. **2019**, 88 (7), 749. https://doi.org/10.1070/RCR4860.

(2) Smith, M.; Kar-Narayan, S. Piezoelectric Polymers: Theory, Challenges and Opportunities. International Materials Reviews **2021**, 0 (0), 1–24. https://doi.org/10.1080/09506608.2021.1915935.

(3) Ionov, L. Hydrogel-Based Actuators: Possibilities and Limitations. Materials Today **2014**, 17 (10), 494–503. https://doi.org/10.1016/j.mattod.2014.07.002.

(4) Le, X.; Lu, W.; Zhang, J.; Chen, T. Recent Progress in Biomimetic Anisotropic Hydrogel Actuators. Advanced Science **2019**, 6 (5), 1801584. https://doi.org/10.1002/advs.201801584.

(5) Lv, H.; Leng, J.; Liu, Y.; Du, S. Shape-Memory Polymer in Response to Solution. Advanced Engineering Materials **2008**, 10 (6), 592–595. https://doi.org/10.1002/adem.200800002.

(6) Du, H.; Zhang, J. Solvent Induced Shape Recovery of Shape Memory Polymer Based on Chemically Cross-Linked Poly(Vinyl Alcohol). Soft Matter **2010**, 6 (14), 3370–3376. https://doi.org/10.1039/B922220K.

(7) Wang, K.; Jia, Y.-G.; Zhao, C.; Zhu, X. X. Multiple and Two-Way Reversible Shape Memory Polymers: Design Strategies and Applications. Progress in Materials Science **2019**, 105, 100572. https://doi.org/10.1016/j.pmatsci.2019.100572.

(8) Pandini, S.; Dioni, D.; Paderni, K.; Messori, M.; Toselli, M.; Bontempi, E.; Riccò, T. The Two-Way Shape Memory Behaviour of Crosslinked Poly(ε-Caprolactone) Systems with Largely Varied Network Density. Journal of Intelligent Material Systems and Structures **2016**, 27 (10), 1388–1403. https://doi.org/10.1177/1045389X15591384.

(9) Dolynchuk, O.; Kolesov, I.; Androsch, R.; Radusch, H.-J. Kinetics and Dynamics of Two-Way Shape-Memory Behavior of Crosslinked Linear High-Density and Short-Chain Branched Polyethylenes with Regard to Crystal Orientation. Polymer **2015**, 79, 146–158. https://doi.org/10.1016/j.polymer.2015.10.017.

(10) Stroganov, V.; Al-Hussein, M.; Sommer, J.-U.; Janke, A.; Zakharchenko, S.; Ionov, L. Reversible Thermosensitive Biodegradable Polymeric Actuators Based on Confined Crystallization. Nano Lett. **2015**, 15 (3), 1786–1790. https://doi.org/10.1021/nl5045023.

(11) Fan, L. F.; Rong, M. Z.; Zhang, M. Q.; Chen, X. D. Dynamic Reversible Bonds Enable External Stress-Free Two-Way Shape Memory Effect of a Polymer Network and the Interrelated Intrinsic Self-Healability of Wider Crack and Recyclability. J. Mater. Chem. A **2018**, 6 (33), 16053–16063. https://doi.org/10.1039/C8TA05751F.

(12) Biswas, A.; Aswal, V. K.; Sastry, P. U.; Rana, D.; Maiti, P. Reversible Bidirectional Shape Memory Effect in Polyurethanes through Molecular Flipping. Macromolecules **2016**, 49 (13), 4889–4897. https://doi.org/10.1021/acs.macromol.6b00536.

(13) Zharinova, E.; Heuchel, M.; Weigel, T.; Gerber, D.; Kratz, K.; Lendlein, A. Water-Blown Polyurethane Foams Showing a Reversible Shape-Memory Effect. Polymers **2016**, 8 (12), 412. https://doi.org/10.3390/polym8120412.

(14) Bothe, M.; Pretsch, T. Bidirectional Actuation of a Thermoplastic Polyurethane Elastomer. Journal of Materials Chemistry A **2013**, 1 (46), 14491–14497. https://doi.org/10.1039/C3TA13414H.

(15) Chung, T.; Romo-Uribe, A.; Mather, P. T. Two-Way Reversible Shape Memory in a Semicrystalline Network. Macromolecules **2008**, 41 (1), 184–192. https://doi.org/10.1021/ma071517z.
(16) Westbrook, K. K.; Parakh, V.; Chung, T.; Mather, P. T.; Wan, L. C.; Dunn, M. L.; Qi, H. J. Constitutive Modeling of Shape Memory Effects in Semicrystalline Polymers With Stretch Induced Crystallization. Journal of Engineering Materials and Technology **2010**, 132 (041010). https://doi.org/10.1115/1.4001964.
(17) Dolynchuk, O.; Kolesov, I.; Radusch, H.-J. Theoretical Description of an Anomalous Elongation During Two-Way Shape-Memory Effect in Crosslinked Semicrystalline Polymers. Macromolecular Symposia **2014**, 346 (1), 48–58. https://doi.org/10.1002/masy.201400065.
(18) Kolesov, I.; Dolynchuk, O.; Jehnichen, D.; Reuter, U.; Stamm, M.; Radusch, H.-J. Changes of Crystal Structure and Morphology during Two-Way Shape-Memory Cycles in Cross-Linked Linear and Short-Chain Branched Polyethylenes. Macromolecules **2015**, 48 (13), 4438–4450. https://doi.org/10.1021/acs.macromol.5b00097.
(19) Huang, M.; Dong, X.; Wang, L.; Zhao, J.; Liu, G.; Wang, D. Two-Way Shape Memory Property and Its Structural Origin of Cross-Linked Poly(ε-Caprolactone). RSC Advances **2014**, 4 (98), 55483–55494. https://doi.org/10.1039/C4RA09385B.
(20) Zare, M.; Prabhakaran, M. P.; Parvin, N.; Ramakrishna, S. Thermally-Induced Two-Way Shape Memory Polymers: Mechanisms, Structures, and Applications. Chemical Engineering Journal **2019**, 374, 706–720. https://doi.org/10.1016/j.cej.2019.05.167.
(21) Bai, Y.; Zhang, X.; Wang, Q.; Wang, T. A Tough Shape Memory Polymer with Triple-Shape Memory and Two-Way Shape Memory Properties. J. Mater. Chem. A **2014**, 2 (13), 4771–4778. https://doi.org/10.1039/C3TA15117D.
(22) Gao, Y.; Liu, W.; Zhu, S. Polyolefin Thermoplastics for Multiple Shape and Reversible Shape Memory. ACS Appl. Mater. Interfaces **2017**, 9 (5), 4882–4889. https://doi.org/10.1021/acsami.6b14728.
(23) Behl, M.; Kratz, K.; Noechel, U.; Sauter, T.; Lendlein, A. Temperature-Memory Polymer Actuators. PNAS **2013**, 110 (31), 12555–12559. https://doi.org/10.1073/pnas.1301895110.
(24) Tamagawa, H. Thermo-Responsive Two-Way Shape Changeable Polymeric Laminate. Materials Letters **2010**, 64 (6), 749–751. https://doi.org/10.1016/j.matlet.2009.12.053.
(25) Chen, S.; Hu, J.; Zhuo, H. Properties and Mechanism of Two-Way Shape Memory Polyurethane Composites. Composites Science and Technology **2010**, 70 (10), 1437–1443. https://doi.org/10.1016/j.compscitech.2010.01.017.
(26) Posada-Murcia, A.; Uribe-Gomez, J. M.; Sommer, J.-U.; Ionov, L. Two-Way Shape Memory Polymers: Evolution of Stress vs Evolution of Elongation. Macromolecules **2021**, 54 (12), 5838–5847. https://doi.org/10.1021/acs.macromol.1c00568.
(27) Nielsen, L. E. Cross-Linking–Effect on Physical Properties of Polymers. Journal of Macromolecular Science, Part C **1969**, 3 (1), 69–103. https://doi.org/10.1080/15583726908545897.
(28) L. Heeley, E.; Kit Poh, C.; Li, W.; Maidens, A.; Bras, W.; P. Dolbnya, I.; J. Gleeson, A.; J. Terrill, N.; A. Fairclough, J. P.; D. Olmsted, P.; I. Ristic, R.; J. Hounslow, M.; J. Ryan, A. Are Metastable, Precrystallisation, Density-Fluctuations a Universal Phenomena? Faraday Discussions **2003**, 122 (0), 343–361. https://doi.org/10.1039/B202680E.

(29) Heeley, E. L.; Maidens, A. V.; Olmsted, P. D.; Bras, W.; Dolbnya, I. P.; Fairclough, J. P. A.; Terrill, N. J.; Ryan, A. J. Early Stages of Crystallization in Isotactic Polypropylene. Macromolecules **2003**, 36 (10), 3656–3665. https://doi.org/10.1021/ma021373i.
(30) Imai, M.; Kaji, K.; Kanaya, T. Orientation Fluctuations of Poly(Ethylene Terephthalate) during the Induction Period of Crystallization. Phys. Rev. Lett. **1993**, 71 (25), 4162–4165. https://doi.org/10.1103/PhysRevLett.71.4162.
(31) Terrill, N. J.; Fairclough, P. A.; Towns-Andrews, E.; Komanschek, B. U.; Young, R. J.; Ryan, A. J. Density Fluctuations: The Nucleation Event in Isotactic Polypropylene Crystallization. Polymer **1998**, 39 (11), 2381–2385. https://doi.org/10.1016/S0032-3861(97)00547-8.
(32) Zhang, J.; Duan, Y.; Sato, H.; Shen, D.; Yan, S.; Noda, I.; Ozaki, Y. Initial Crystallization Mechanism of Isotactic Polystyrene from Different States. J. Phys. Chem. B **2005**, 109 (12), 5586–5591. https://doi.org/10.1021/jp0449004.
(33) Essery, R. L. H.; Ball, R. C. Anisotropic Spinodal Decomposition. EPL **1991**, 16 (4), 379–384. https://doi.org/10.1209/0295-5075/16/4/011.
(34) Zhang, Y.; Huo, H.; Li, J.; Shang, Y.; Chen, Y.; S. Funari, S.; Jiang, S. Crystallization Behavior of Poly(ε-Caprolactone) and Poly (ε-Caprolactone)/LiClO 4 Complexes from the Melt. CrystEngComm **2012**, 14 (23), 7972–7980. https://doi.org/10.1039/C2CE25126D.
(35) Kamal, T.; Shin, T. J.; Park, S.-Y. Uniaxial Tensile Deformation of Poly(ε-Caprolactone) Studied with SAXS and WAXS Techniques Using Synchrotron Radiation. Macromolecules **2012**, 45 (21), 8752–8759. https://doi.org/10.1021/ma301714f.
(36) McCrone, W. C.; McCrone, L. B.; Delly, J. G. Polarized Light Microscopy; 19780000;19840000.
(37) Guinier, A.; Fournet, G. Small-Angle Scattering of X-Rays; Wiley, 1955.
(38) Förster, S.; Timmann, A.; Konrad, M.; Schellbach, C.; Meyer, A.; Funari, S. S.; Mulvaney, P.; Knott, R. Scattering Curves of Ordered Mesoscopic Materials. J. Phys. Chem. B **2005**, 109 (4), 1347–1360. https://doi.org/10.1021/jp0467494.
(39) Biehl, R. Jscatter, a Program for Evaluation and Analysis of Experimental Data. PLOS ONE **2019**, 14 (6), e0218789. https://doi.org/10.1371/journal.pone.0218789.

For Table Of Contents Use Only

TOC Image